JACS
JOURNAL OF THE AMERICAN CHEMICAL SOCIETY

Communication

pubs.acs.org/JACS

Embryonic Growth of Face-Center-Cubic Silver Nanoclusters Shaped in Nearly Perfect Half-Cubes and Cubes

Huayan Yang,[†] Juanzhu Yan,[†] Yu Wang,[†] Haifeng Su,[†] Lars Gell,[‡] Xiaojing Zhao,[†] Chaofa Xu,[†] Boon K. Teo,*[,†] Hannu Häkkinen,*[,‡] and Nanfeng Zheng*[,†]

[†]State Key Laboratory for Physical Chemistry of Solid Surfaces, Collaborative Innovation Center of Chemistry for Energy Materials, and Engineering Research Center for Nano-Preparation Technology of Fujian Province, College of Chemistry and Chemical Engineering, Xiamen University, Xiamen 361005, China

[‡]Departments of Physics and Chemistry, Nanoscience Center, University of Jyväskylä, FI-40014 Jyväskylä, Finland

Supporting Information

ABSTRACT: Demonstrated herein are the preparation and crystallographic characterization of the family of fcc silver nanoclusters from Nichol's cube to Rubik's cube and beyond via ligand-control (thiolates and phosphines in this case). The basic building block is our previously reported fcc cluster $[Ag_{14}(SPhF_2)_{12}(PPh_3)_8]$ (**1**). The metal frameworks of $[Ag_{38}(SPhF_2)_{26}(PR'_3)_8]$ ($\mathbf{2^2}$) and $[Ag_{63}(SPhF_2)_{36}(PR'_3)_8]^+$ ($\mathbf{2^3}$), where $HSPhF_2$ = 3,4-difluorothiophenol and R′ = alkyl/aryl, are composed of 2 × 2 = 4 and 2 × 2 × 2 = 8 metal cubes of **1**, respectively. All serial clusters share similar surface structural features. The thiolate ligands cap the six faces and the 12 edges of the cube (or half cube) while the phosphine ligands are terminally bonded to its eight corners. On the basis of the analysis of the crystal structures of **1**, $\mathbf{2^2}$, and $\mathbf{2^3}$, we predict the next "cube of cubes" to be $Ag_{172}(SR)_{72}(PR'_3)_8]$ ($\mathbf{3^3}$), in the evolution of growth of this cluster sequence.

Atomically precise metal nanoclusters have been the sought-after nanoparticles of critical importance in the development of nanoscience and nanotechnology.[1−21] In the field of metal nanomaterials, controlling the shapes and structures of metal crystals has proved to be a powerful means for tailoring their properties for a wide of applications, including, but not limited to, plasmonics, catalysis, surface enhanced Raman scattering (SERS), sensing and imaging.[22−27] To achieve desirable shapes of metal nanocrystals, significant efforts have been made in developing new strategies for their shape-controlled synthesis.[26−37] Among these approaches, the use of specific capping ligands to control the exposed surface of metal nanocrystals is an effective strategy.[37−41] Though a wide variety of capping agents have been used in controlling the shapes of metal nanocrystals, it is still unclear how these capping agents work in terms of their binding capabilities and selectivities toward a specific metal surface and their effects on the size and shape of the resulting nanocrystals. Due to their nature of 100% monodispersity at the molecular level, atomically precise metal nanoclusters are readily crystallized into single crystals for resolving their total structures, including the detailed binding modes of surface ligands.[1−18] Systematic investigations of the structures of metal nanoclusters can thus shed light on the atomic details of the early, or embryonic stages of the growth of metal particles, thereby allowing studies of how capping agents control the shape evolution process of metal nanocrystals.

We report herein the synthesis and single-crystal structures of two new face-center-cubic (fcc) silver nanoclusters, namely, $[Ag_{38}(SPhF_2)_{26}(P^nBu_3)_8]$ ($\mathbf{2^2}$) and $[Ag_{63}(SPhF_2)_{36}(P^nBu_3)_8]^+$ ($\mathbf{2^3}$). The metal frameworks can be likened to Nichol's half ($\mathbf{2^2}$) and full ($\mathbf{2^3}$) cubes, respectively, as depicted in Figure 1. The basic building block is our previously reported fcc cluster $[Ag_{14}(SPhF_2)_{12}(PPh_3)_8]$ (**1**, Figure 1a).[42] Thus, the metal frameworks of $\mathbf{2^2}$ and $\mathbf{2^3}$ are composed of 2 × 2 = 4 and 2 × 2 × 2 = 8 metal cubes of **1**, respectively. It occurs to us that these atomically precise molecular nanosized metal clusters are early members of a growth sequence, from **1** to $\mathbf{2^2}$ to $\mathbf{2^3}$ to $\mathbf{3^3}$ to $\boldsymbol{n^3}$, based on fcc metal cubes (cf. Figure 1d−g). Cluster $\mathbf{3^3}$ is the renowned Rubik's cube composed of 3 × 3 × 3 = 27 basic cubes that mesmerized the world in the 1980s. (Hereafter, the

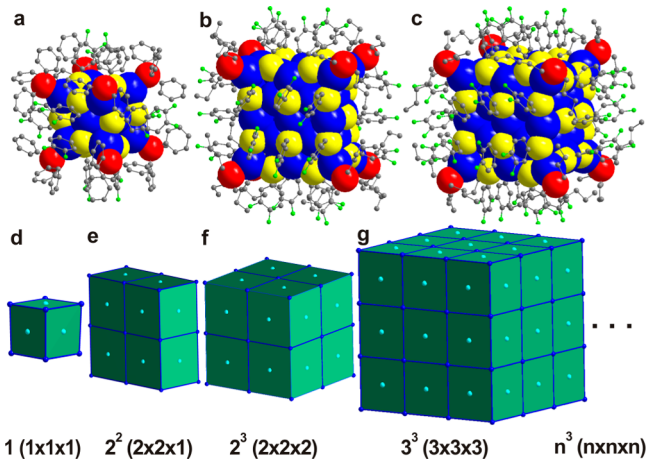

Figure 1. Crystallographic structures of Ag cubes and their corresponding models: (a) $[Ag_{14}(SPhF_2)_{12}(PPh_3)_8]$ (**1**); (b) $[Ag_{38}(SPhF_2)_{26}(P^nBu_3)_8]$ ($\mathbf{2^2}$); (c) $[Ag_{63}(SPhF_2)_{36}(P^nBu_3)_8]^+$ ($\mathbf{2^3}$) clusters. (d−g) are the idealized fcc close-packing growth sequence of corresponding cubes. Color codes: blue and light blue sphere, Ag; red sphere, P; yellow sphere, S; green, F; gray, C. All hydrogen atoms are omitted for clarity.

Received: September 30, 2016
Published: December 19, 2016

DOI: 10.1021/jacs.6b10053
J. Am. Chem. Soc. 2017, 139, 31−34

formular designators **1**, $\mathbf{2}^2$, $\mathbf{2}^3$, and $\mathbf{3}^3$ will be used to represent the corresponding metal frameworks as well.) The key in the synthetic strategy is to recognize that the size, morphology and structure of the resulting clusters are controlled by the surface ligands (thiolates and phosphines in this case) as we shall describe herein.

The molecular structures of **1**, $\mathbf{2}^2$, and $\mathbf{2}^3$ are shown in Figure 1, respectively. The eight fcc units in $\mathbf{2}^3$ are arranged in a cube of frequency two (n = 2) whereas $\mathbf{2}^2$ is simply half of $\mathbf{2}^3$, with four fcc units arranged in a square pattern. Interestingly, the surface ligands share the following common binding features among **1**, $\mathbf{2}^2$, and $\mathbf{2}^3$: the thiolate ligands cap the six faces and the 12 edges of the cube (or half cube) while the phosphine ligands are terminally bonded to the cube's (or half-cube's) eight corners.

The cluster $\mathbf{2}^2$ was synthesized by chemical reduction of silver tetrafluoroborate ($AgBF_4$) with an aqueous solution of $NaBH_4$ in the presence of thiol and phosphine in a mixed solvent of dichloromethane and methanol at 0 °C in an ice bath. In the synthesis of $\mathbf{2}^3$, tetrabutylammonium tetraphenylborate ($^n Bu_4N{\cdot}BPh_4$) was introduced as counterion (see Supporting Information for more details). Introducing large counterions in the synthesis helped to stabilize charged nanoclusters, thereby facilitating the crystallization process as well as enhancing the yields (Figure S1). Single crystals of $\mathbf{2}^2$ and $\mathbf{2}^3$ suitable for X-ray single-crystal diffraction studies (Tables S1–S4) were obtained by layering hexane onto the CH_2Cl_2 solutions and freezing crystallization at 4 °C, respectively.

As depicted in Figures 2a and S2, the metal framework of **1** has a simple fcc structure. The structure can be described as an

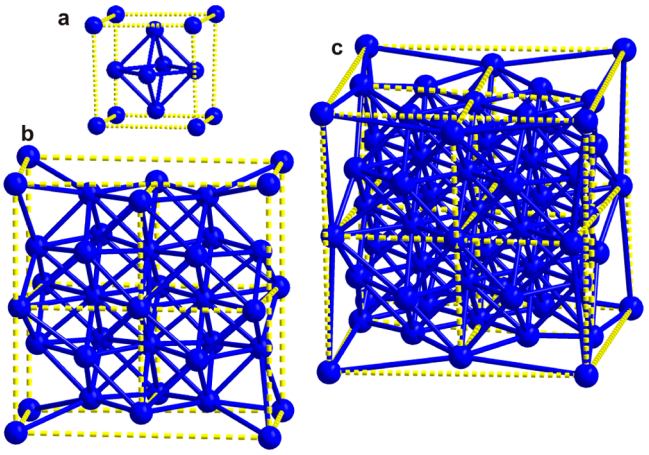

Figure 2. Metal frameworks of different cube-like Ag nanoclusters: (a) $[Ag_{14}(SPhF_2)_{12}(PPh_3)_8]$ (**1**), (b) $[Ag_{38}(SPhF_2)_{26}(P^nBu_3)_8]$ ($\mathbf{2}^2$), and (c) $[Ag_{63}(SPhF_2)_{36}(P^nBu_3)_8]^+$ ($\mathbf{2}^3$). Color codes: blue sphere, Ag. All phosphorus, sulfur, carbon, fluorine, and hydrogen atoms are omitted for clarify.

octacapped octahedron of an $Ag_6@Ag_8$ cluster with the 12 bridging thiolate ligands situated at the midpoints of the 12 edges of the outer Ag_8 cube and the eight phosphines ligated to the Ag atoms at the corners of the cube. Alternatively, it can be described as an octahedral Ag_6^{4+} kernel encapsulated by eight cubically arranged $[Ag(SPhF_2)_3PPh_3]$ tetrahedra sharing S atoms (from $SPhF_2$).

As shown in Figures 2b and S3, the metal framework of $\mathbf{2}^2$ is formed by four fcc units arranged in a square fashion by sharing faces. The long and short edge lengths of the metal framework are 9.633 and 5.017 Å, respectively. The Ag–Ag distances in $\mathbf{2}^2$ range from 2.747 to 4.069 Å (Table S5) with an average of 3.151 Å, which is shorter than the average Ag–Ag distance of 3.333 Å in **1**. As illustrated in Figures 2c and S4, the metal framework of $\mathbf{2}^3$ is formed by eight fcc units arranged to form a cube of frequency two by sharing faces. It can also be considered as two $\mathbf{2}^2$ fused together by sharing the large square (of frequency two). The edge length of the cubic $\mathbf{2}^3$ framework is 9.583 Å, somewhat shorter than the long edge (9.633 Å) of the framework of $\mathbf{2}^2$. The Ag–Ag distances in $\mathbf{2}^3$ range from 2.880 to 3.996 Å with an average of 3.048 Å. The average Ag–Ag distance of $\mathbf{2}^3$ is also slightly shorter than the average Ag–Ag distance of $\mathbf{2}^2$, which is the reason for the shorter edge of the Ag_{63} framework.

In addition to the nearly identical fcc packing of Ag atoms in their metal frameworks, as shown as in Figures 3 and S3–S5, all

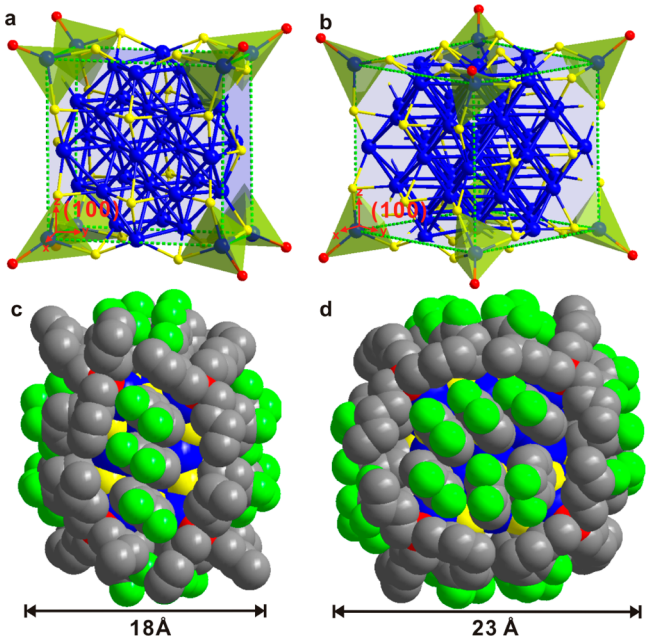

Figure 3. Ligand shell and space-filling structures of $[Ag_{38}(SPhF_2)_{26}(P^nBu_3)_8]$ (a,c) and $[Ag_{63}(SPhF_2)_{36}(P^nBu_3)_8]^+$ (b,d). Color codes: blue sphere, Ag; yellow sphere, S; red sphere, P; green, F; gray sphere, C. All hydrogen atoms are omitted for clarify.

three clusters share similar surface structural features. The thiolate ligands on surfaces can be classified into two groups. On the (100) faces, each thiolate is four-coordinated to the four Ag atoms of rhombic Ag_4 face. On the edges, the thiolates are three-coordinated to three Ag atoms, one each from the nearest corner, edge, and face. For $\mathbf{2}^2$ and $\mathbf{2}^3$, the average Ag–S bonds are 2.583 and 2.587 respectively, which are slightly longer than the Ag–S bonds in $[M_{12}Ag_{32}(SR)_{30}]^{4-}$ (M = Au or Ag) clusters (2.54–2.57 Å).[6] There are eight phosphine ligands bonded to the eight Ag atoms situated at the corners of the half cube of $\mathbf{2}^2$ or the full cube of $\mathbf{2}^3$. The average Ag–P bonds are 2.416 and 2.392 for $\mathbf{2}^2$ and $\mathbf{2}^3$, respectively. Each of the corner Ag atoms is further coordinated by three bridging thiolate ligands, making them four-coordinated. The Ag atoms on the edges are three-coordinated by three thiolates, and the Ag atoms on the faces are coordinated by two thiolate ligands. It should be noted that, in the case of $\mathbf{2}^2$, clusters with either PPh_3 or P^nBu_3 coordinated

DOI: 10.1021/jacs.6b10053
J. Am. Chem. Soc. 2017, 139, 31–34

to their eight corner Ag atoms had been synthesized (Figures S3 and S5).

It is interesting to predict the next "cube of cubes" in this series. Based on the above analysis of the crystal structures of **1**, $\mathbf{2}^2$, and $\mathbf{2}^3$, the next member is predicted to be of frequency three, designated as $\mathbf{3}^3$, with $3 \times 3 \times 3 = 27$ basic fcc units. The generating functions for this particular sequence of fcc metal clusters, of the general formulas $[M_x(SR)_y(PR'_3)_8]^z$ clusters with face-centered cubes of frequency n are $x = (n+1)(4n^2+2n+1)$; $y = 6n(n+1)$; and $z = +1$ for n = even and $z = 0$ for n = odd. Based on these equations, the formula of $\mathbf{3}^3$ (Rubik's cube cluster) is predicted to be $[Ag_{172}(SR)_{72}(PR_3')_8]$. The yet-unknown Rubik's cube structure is shown in Figure S6.

As shown in Figure 4, UV−vis spectra of $\mathbf{2}^2$ and $\mathbf{2}^3$ in CH_2Cl_2 exhibit multi-band broad optical absorptions: for $\mathbf{2}^2$, three peaks

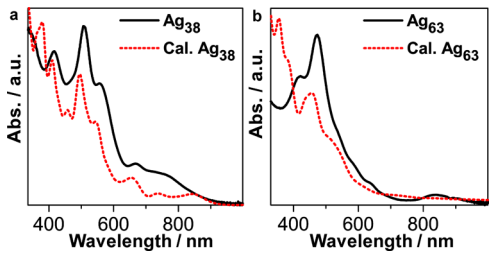

Figure 4. Comparison of experimental and theoretically calculated UV−vis absorption spectra of $\mathbf{2}^2$ (a) and $\mathbf{2}^3$ (b).

at 413, 507, 563 nm (with four shoulders at 351, 468, 609, and 767 nm). And for $\mathbf{2}^3$, four peaks at 325, 415, 470, and 840 nm (with one shoulder at 580 nm). In contrast, **1** displays only two shoulder bands at 368 and 530 nm.[42] According to the widespread rule to count the free metal electrons in ligand-protected metal clusters,[43] clusters **1**, $\mathbf{2}^2$ and (cationic) $\mathbf{2}^3$ are 2, 12, and 26 free-electron systems. Cluster **1** is a two-electron superatom, and its optical absorption has been analyzed previously in terms of superatom 1S to 1P and ligand-to-ligand transitions.[44]

Here, the ground state electronic structure and excited-state absorption of $\mathbf{2}^2$ and $\mathbf{2}^3$ were studied by using linear-response time-dependent density functional theory (LR-TDDFT) (see Supporting Information for computational details). The full ligand shell was treated with experimentally used ligands in the calculations. The cluster structures were relaxed to the theoretical energy minimum starting from the crystal structure without any symmetry constraints. The theoretical minimum energy structure for both clusters follows very closely to the experimental structure. The ground state calculations reveal that $\mathbf{2}^2$ is electronically a rather stable cluster with an energy gap of 0.67 eV between the highest occupied molecular orbital (HOMO) and lowest unoccupied molecular orbital (LUMO) (see Figure S7). It is not immediately obvious why such a clear energy gap is stabilized for 12 free electrons of the cluster, although 12 can be an electronic magic number for a circularly symmetric, square-box-symmetric or triangular-symmetric, strictly 2D or quasi-2D system.[45] Here we note that the flat box-shape of $\mathbf{2}^2$ bears some similarity to oblate symmetric 2D systems. On the contrary, calculations reveal that $\mathbf{2}^3$ has a tiny (0.07 eV) HOMO−LUMO energy gap in the cationic state of the cluster (Figure S8). The anionic state would have a larger gap of about 0.3 eV. In that system, the stabilization is not of electronic origin and must then primarily come from the steric protection of the ligand layer and atom-packing in the near-perfect cube. In this regard, $\mathbf{2}^3$ exhibits a better stability than $\mathbf{2}^2$ in 1,2-dichloroethane at 50 °C in air (Figure S9).

In conclusion, two face-center-cubic (fcc) silver nanoclusters, $[Ag_{38}(SPhF_2)_{26}(P^nBu_3)_8]$ ($\mathbf{2}^2$) and $[Ag_{63}(SPhF_2)_{36}(P^nBu_3)_8]^+$ ($\mathbf{2}^3$) were synthesized via ligand-control. These two nanoclusters are composed of the basic fcc Ag_{14} unit found in $[Ag_{14}(SPhF_2)_{12}(PPh_3)_8]$ (**1**).[42] Thus, $\mathbf{2}^2$ is a 2×2 half cube whereas $\mathbf{2}^3$ is a $2 \times 2 \times 2$ full cube. It has been well-documented that ligands play important roles in the shape-controlled synthesis of metal nanocrystals. Together with the recent work by Bakr,[46] this work sheds light on how ligands influence the nucleation and growth process of the metal nanocrystals. For the formation of a $[Ag_x(SR)_y(PR'_3)_8]^z$ cube-shaped nanocluster, it is essential to have the selective binding of thiolate ligands on its six faces and 12 edges, and monodendate phosphine ligands on its eight corners. The ratio of ligands to Ag helps to control the size of the resulting nanoclusters. Decreasing the ratio would lead to the formation of nanocubes of increasing size. The structures reported in this work also provide well-defined structure models for specific surface modification of faceted fcc metal nanocrystals.

■ ASSOCIATED CONTENT

Supporting Information

The Supporting Information is available free of charge on the ACS Publications website at DOI: 10.1021/jacs.6b10053.

Experimental details, computational details, analysis of the cluster electronic structure (PDF)

Crystallographic structure and data for $C_{252}H_{286}Ag_{38}F_{52}P_8S_{26}$, $4(CH_2Cl_2)$ (CIF)

Crystallographic structure and data for $C_{300}H_{198}Ag_{38}F_{52}P_8S_{26}$ (CIF)

Crystallographic structure and data for $C_{318}H_{324}Ag_{63}F_{72}P_8S_{36}$, $C_{24}H_{20}B$ (CIF)

Crystallographic structure and data for $Ag_{63}C_{312}F_{72}P_8S_{36}$, Br (CIF)

■ AUTHOR INFORMATION

Corresponding Authors

*N.F.Z. nfzheng@xmu.edu.cn

*B.K.T. boonkteo@xmu.edu.cn

*H.H. hannu.j.hakkinen@jyu.fi

ORCID

Hannu Häkkinen: 0000-0002-8558-5436

Nanfeng Zheng: 0000-0001-9879-4790

Author Contributions

H.Y. and J.Y. contributed equally to this work.

Notes

The authors declare no competing financial interest.

■ ACKNOWLEDGMENTS

We thank the MOST of China (2015CB932303) and the NNSF of China (21420102001, 21131005, 21390390, 21227001, 21333008) for financial support. The work in University of Jyväskylä was supported by the Academy of Finland (266492 and H.H. Academy Professorship). The computations were made at the CSC − the Finnish IT Center for Science in Espoo, Finland.

DOI: 10.1021/jacs.6b10053
J. Am. Chem. Soc. 2017, 139, 31−34

REFERENCES

(1) Jadzinsky, P. D.; Calero, G.; Ackerson, C. J.; Bushnell, D. A.; Kornberg, R. D. *Science* **2007**, *318*, 430.
(2) Heaven, M. W.; Dass, A.; White, P. S.; Holt, K. M.; Murray, R. W. *J. Am. Chem. Soc.* **2008**, *130*, 3754.
(3) Zhu, M.; Aikens, C. M.; Hollander, F. J.; Schatz, G. C.; Jin, R. *J. Am. Chem. Soc.* **2008**, *130*, 5883.
(4) Liu, C. W.; Li, T.; Li, G.; Nobusada, K.; Zeng, C.; Pang, G.; Rosi, N. L.; Jin, R. C. *Angew. Chem., Int. Ed.* **2015**, *54*, 9826.
(5) Yang, H. Y.; Wang, Y.; Chen, X.; Zhao, X. J.; Gu, L.; Huang, H. Q.; Yan, J. Z.; Xu, C. F.; Li, G.; Wu, J. C.; Edwards, A. J.; Dittrich, B.; Tang, Z. C.; Wang, D. D.; Lehtovaara, L.; Häkkinen, H.; Zheng, N. F. *Nat. Commun.* **2016**, *7*, 12809.
(6) Yang, H. Y.; Wang, Y.; Huang, H. Q.; Gell, L.; Lehtovaara, L.; Malola, S.; Häkkinen, H.; Zheng, N. F. *Nat. Commun.* **2013**, *4*, 2422.
(7) Desireddy, A.; Conn, B. E.; Guo, J.; Yoon, B.; Barnett, R. N.; Monahan, B. M.; Kirschbaum, K.; Griffith, W. P.; Whetten, R. L.; Landman, U.; Bigioni, T. P. *Nature* **2013**, *501*, 399.
(8) Joshi, C. P.; Bootharaju, M. S.; Alhilaly, M. J.; Bakr, O. M. *J. Am. Chem. Soc.* **2015**, *137*, 11578.
(9) Li, G.; Jin, R. *Acc. Chem. Res.* **2013**, *46*, 1749.
(10) Soldan, G.; Aljuhani, M. A.; Bootharaju, M. S.; AbdulHalim, L. G.; Parida, M. R.; Emwas, A.; Mohammed, O. F.; Bakr, O. M. *Angew. Chem.* **2016**, *128*, 5843.
(11) Yu, Y.; Luo, Z. T.; Chevrier, D. M.; Leong, D. T.; Zhang, P.; Jiang, D. E.; Xie, J. P. *J. Am. Chem. Soc.* **2014**, *136*, 1246.
(12) AbdulHalim, L. G.; Bootharaju, M. S.; Tang, Q.; Del Gobbo, S.; AbdulHalim, R. G.; Eddaoudi, M.; Jiang, D. E.; Bakr, O. M. *J. Am. Chem. Soc.* **2015**, *137*, 11970.
(13) Shichibu, Y.; Negishi, Y.; Watanabe, T.; Chaki, N. K.; Kawaguchi, H.; Tsukuda, T. *J. Phys. Chem. C* **2007**, *111*, 7845.
(14) Kobayashi, N.; Kamei, Y.; Shichibu, Y.; Konishi, K. *J. Am. Chem. Soc.* **2013**, *135*, 16078.
(15) Wan, X.-K.; Yuan, S.-F.; Lin, Z.-W.; Wang, Q.-M. *Angew. Chem., Int. Ed.* **2014**, *53*, 2923.
(16) Wang, S.; Jin, S.; Yang, S.; Chen, S.; Song, Y.; Zhang, J.; Zhu, M. *Sci. Adv.* **2015**, *1*, e1500441.
(17) Dass, A.; Theivendran, S.; Nimmala, P. R.; Kumara, C.; Jupally, V. R.; Fortunelli, A.; Sementa, L.; Barcaro, G.; Zuo, X.; Noll, B. C. *J. Am. Chem. Soc.* **2015**, *137*, 4610.
(18) Wang, Y.; Wan, X. K.; Ren, L. T.; Su, H. F.; Li, G.; Malola, S.; Lin, S. C.; Tang, Z. C.; Häkkinen, H.; Teo, B. K.; Wang, Q. M.; Zheng, N. F. *J. Am. Chem. Soc.* **2016**, *138*, 3278.
(19) Niihori, Y.; Matsuzaki, M.; Pradeep, T.; Negishi, Y. *J. Am. Chem. Soc.* **2013**, *135*, 4946.
(20) Dhayal, R. S.; Lin, Y.; Liao, J.; Chen, Y.; Liu, Y.; Chiang, M.; Kahlal, S.; Saillard, J.; Liu, C. W. *Chem. - Eur. J.* **2016**, *22*, 9943.
(21) Dhayal, R. S.; Liao, J.; Liu, Y.; Chiang, M.; Kahlal, S.; Saillard, J.; Liu, C. W. *Angew. Chem., Int. Ed.* **2015**, *54*, 3702.
(22) Lu, L.; Luo, Z.; Xu, T.; Yu, L. *Nano Lett.* **2013**, *13*, 59.
(23) Linic, S.; Aslam, U.; Boerigter, C.; Morabito, M. *Nat. Mater.* **2015**, *14*, 567.
(24) Lee, I.; Delbecq, F.; Morales, R.; Albiter, M. A.; Zaera, F. *Nat. Mater.* **2009**, *8*, 132.
(25) Narayanan, R.; El-Sayed, M. A. *Nano Lett.* **2004**, *4*, 1343.
(26) Xia, Y.; Xiong, Y.; Lim, B.; Skrabalak, S. E. *Angew. Chem., Int. Ed.* **2009**, *48*, 60.
(27) Yin, A.; Liu, W.; Ke, J.; Zhu, W.; Gu, J.; Zhang, Y.; Yan, C. *J. Am. Chem. Soc.* **2012**, *134*, 20479.
(28) Zhang, J.; Du, J.; Han, B.; Liu, Z.; Jiang, T.; Zhang, Z. *Angew. Chem.* **2006**, *118*, 1134.
(29) Wei, Z.; Matsui, H. *Nat. Commun.* **2014**, *5*, 3870.
(30) Skrabalak, S. E.; Au, L.; Li, X.; Xia, Y. *Nat. Protoc.* **2007**, *2*, 2182.
(31) Anker, J. N.; Hall, W. P.; Lyandres, O.; Shah, N. C.; Zhao, J.; Van Duyne, R. P. *Nat. Mater.* **2008**, *7*, 442.
(32) Xia, Y.; Xia, X.; Peng, H. *J. Am. Chem. Soc.* **2015**, *137*, 7947.
(33) Yu, D.; Yam, V. W. *J. Am. Chem. Soc.* **2004**, *126*, 13200.
(34) Puntes, V. F.; Krishnan, K. M.; Alivisatos, A. P. *Science* **2001**, *291*, 2115.
(35) Negishi, Y.; Nobusada, K.; Tsukuda, T. *J. Am. Chem. Soc.* **2005**, *127*, 5261.
(36) Shichibu, Y.; Suzuki, K.; Konishi, K. *Nanoscale* **2012**, *4*, 4125.
(37) Chen, M.; Wu, B. H.; Yang, J.; Zheng, N. F. *Adv. Mater.* **2012**, *24*, 862.
(38) Zeng, J.; Zheng, Y.; Rycenga, M.; Tao, J.; Li, Z.; Zhang, Q.; Zhu, Y.; Xia, Y. *J. Am. Chem. Soc.* **2010**, *132*, 8552.
(39) Biacchi, A. J.; Schaak, R. E. *ACS Nano* **2015**, *9*, 1707.
(40) Xiang, H.; Kang, J.; Wei, S.; Kim, Y.; Curtis, C.; Blake, D. *J. Am. Chem. Soc.* **2009**, *131*, 8522.
(41) Grzelczak, M.; Perez-Juste, J.; Mulvaney, P.; Liz-Marzan, L. M. *Chem. Soc. Rev.* **2008**, *37*, 1783.
(42) Yang, H. Y.; Lei, J.; Wu, B. H.; Wang, Y.; Zhou, M.; Xia, A. D.; Zheng, L. S.; Zheng, N. F. *Chem. Commun.* **2013**, *49*, 300.
(43) Walter, M.; Akola, J.; Lopez-Acevedo, O.; Jadzinsky, P. D.; Calero, G.; Ackerson, C. J.; Whetten, R. L.; Grönbeck, H.; Häkkinen, H. *Proc. Natl. Acad. Sci. U. S. A.* **2008**, *105*, 9157.
(44) Gell, L.; Lehtovaara, L.; Häkkinen, H. *J. Phys. Chem. A* **2014**, *118*, 8351.
(45) Häkkinen, H. *Adv. Phys. X* **2016**, *1*, 467.
(46) Alhilaly, M. J.; Bootharaju, M. S.; Joshi, C. P.; Besong, T. M.; Emwas, A.-H.; Juarez-Mosqueda, R.; Kaappa, S.; Malola, S.; Adil, K.; Shkurenko, A.; Hakkinen, H.; Eddaoudi, M.; Bakr, O. M. *J. Am. Chem. Soc.* **2016**, *138*, 14727.

DOI: 10.1021/jacs.6b10053
J. Am. Chem. Soc. 2017, 139, 31−34